Role of Subsurface Physics in the Assimilation of Surface Soil Moisture Observations

SUJAY V. KUMAR

Science Applications International Corporation, Beltsville, and Hydrological Sciences Branch, NASA Goddard Space Flight Center, Greenbelt, Maryland

ROLF H. REICHLE AND RANDAL D. KOSTER

Global Modeling and Assimilation Office, NASA Goddard Space Flight Center, Greenbelt, Maryland

WADE T. CROW

Hydrology and Remote Sensing Laboratory, Agriculture Research Service, U.S. Department of Agriculture, Beltsville, Maryland

CHRISTA D. PETERS-LIDARD

Hydrological Sciences Branch, NASA Goddard Space Flight Center, Greenbelt, Maryland

(Manuscript received 4 December 2008, in final form 3 June 2009)

ABSTRACT

Root-zone soil moisture controls the land–atmosphere exchange of water and energy, and exhibits memory that may be useful for climate prediction at monthly scales. Assimilation of satellite-based surface soil moisture observations into a land surface model is an effective way to estimate large-scale root-zone soil moisture. The propagation of surface information into deeper soil layers depends on the model-specific representation of subsurface physics that is used in the assimilation system. In a suite of experiments, synthetic surface soil moisture observations are assimilated into four different models [Catchment, Mosaic, Noah, and Community Land Model (CLM)] using the ensemble Kalman filter. The authors demonstrate that identical twin experiments significantly overestimate the information that can be obtained from the assimilation of surface soil moisture observations. The second key result indicates that the potential of surface soil moisture assimilation to improve root-zone information is higher when the surface–root zone coupling is stronger. The experiments also suggest that (faced with unknown true subsurface physics) overestimating surface–root zone coupling in the assimilation system provides more robust skill improvements in the root zone compared with underestimating the coupling. When CLM is excluded from the analysis, the skill improvements from using models with different vertical coupling strengths are comparable for different subsurface truths. Last, the skill improvements through assimilation were found to be sensitive to the regional climate and soil types.

1. Introduction

Soil moisture (sm) plays an important role in controlling evaporation, plant transpiration, infiltration, and runoff, and consequently in modulating the partitioning of water and energy fluxes across the land–atmosphere interface. Moreover, root-zone soil moisture provides a critical memory function in the climate system at monthly time scales. Characterization of soil moisture in the root zone is therefore important for many applications, including agricultural and water resources management, short- and medium-term meteorological and climate studies, and flood/drought forecasting. (Koster et al. 2004; Oglesby 1991; Chen and Avissar 1994; Trier et al. 2004; Kumar et al. 2007).

Using observation-based surface meteorological data to drive land surface models in an uncoupled manner is a common approach used to generate spatially and temporally continuous estimates of land surface states, including soil moisture (Mitchell et al. 2004; Rodell et al. 2004; Kumar et al. 2006). The estimates from these models, however, are uncertain because of errors in

Corresponding author address: S. V. Kumar, Hydrological Sciences Branch, Code 614.3, Greenbelt, MD 20771.
E-mail: sujay.v.kumar@nasa.gov

DOI: 10.1175/2009JHM1134.1

© 2009 American Meteorological Society

model parameters and forcing inputs and because of deficiencies in the model representation of land surface processes. Indirect estimates of surface soil moisture for the top 1–5 cm of the soil column are also available from satellite remote sensing observations (Schmugge et al. 1980; Engman and Gurney 1991; Jackson 1993; Njoku and Entekhabi 1995). Such satellite retrievals, however, are subject to measurement noise and errors in retrieval models, are limited to the top few millimeters or centimeters of soil, and do not provide complete spatial and temporal coverage. An effective way to attenuate model and observational errors and produce superior estimates of soil moisture states is to constrain the land model predictions with satellite observations of surface soil moisture through data assimilation methods. Such methods vertically extrapolate temporally intermittent surface retrievals and produce estimates of root-zone soil moisture that are generally superior to estimates from land surface models alone (Reichle et al. 2007).

Various computational techniques have been used to derive estimates of the soil moisture profile from surface measurements—including regression techniques, inversion of radiative transfer methods, parametric profile models, and data assimilation methods—in conjunction with physical models (Jackson 1986; Kostov and Jackson 1993; Jackson 1993; Entekhabi et al. 1994; Li and Islam 2002). Among these efforts, the integrated use of data assimilation and hydrological models has been cited as the most promising approach. Some early feasibility and field-scale studies demonstrated improvements in near-surface and bulk subsurface soil moisture through data assimilation (Calvet et al. 1998; Heathman et al. 2003; Montaldo et al. 2001; Reichle et al. 2002a; Walker et al. 2001, 2002; Reichle and Koster 2003). Improvements in surface and root-zone soil moisture through data assimilation of global satellite retrievals have recently been demonstrated (Reichle and Koster 2005; Reichle et al. 2007; Drusch 2007). Taken together, these studies describe the development of advanced methodologies and establish the potential of near-surface soil moisture data assimilation to infer estimates of subsurface profiles.

Data assimilation techniques rely on the inherent surface–root zone connection to propagate surface information to deeper soil layers. The subsurface physics used in the land surface model, therefore, is an important factor in determining the strength and validity of the downward propagation of surface information. In this article, we evaluate how the use of different subsurface physics affects the data assimilation performance, especially in the root-zone assimilation products. The experiment is conducted with four land surface models (LSMs) of varying complexity [Catchment (Cat), Mosaic (Mos), Noah, and Community Land Model (CLM)]—each applying different subsurface physics schemes. As we will show, the Catchment and Mosaic LSMs exhibit particularly strong soil moisture coupling between its surface and root zones, whereas Noah and CLM show successively weaker connections between the surface and root zone.

Synthetic observations generated from control integrations using each of the four models are reassimilated into the same model and cross-assimilated into each of the other three models. This setup leads to a suite of experiments in which each LSM is provided with different sets of observations. Depending on the surface–root zone (vertical) coupling strength of the LSM, the information from surface observations is vertically propagated differently for each LSM during data assimilation. The evaluation of the assimilation products reveals how well each LSM performs in a data assimilation system under varying assumptions of vertical coupling strength. It must be stressed that the intent of the experiments is not to judge the veracity of the LSMs to reproduce large-scale land surface processes and conditions as they occur in nature. Again, our goal is to demonstrate how the LSMs perform in a data assimilation system under many different representations of possible true land surface processes. In particular, we aim to quantify how the strength of the vertical connection between the surface and root zone (in the assimilation model or in the assumed "truth") affects the efficiency and veracity of information transfer into the root zone through assimilation. Understanding this transfer is key to exploiting the information content of the next generation of satellite soil moisture retrievals from the Soil Moisture and Ocean Salinity (National Research Council 2007) and the Soil Moisture Active and Passive (Kerr et al. 2001) satellite missions to be launched in 2009 and 2013, respectively.

2. Approach

a. Land surface models

This study is conducted using the Land Information System (LIS) data assimilation test bed, which provides a framework for the integrated use of several community LSMs, observation types, and sequential data assimilation algorithms (Kumar et al. 2008b). The interoperable features of the LIS framework (Kumar et al. 2006; Peters-Lidard et al. 2007; Kumar et al. 2008a) make it an ideal platform for conducting the intercomparison experiments presented here.

The suite of experiments presented in this article is conducted four community LSMs: (i) National Aeronautics and Space Administration (NASA) Catchment LSM (Koster et al. 2000); (ii) Mosaic LSM (Koster

and Suarez 1996); (iii) Noah LSM (Ek et al. 2003); and (iv) CLM, version 2.0 (Dai et al. 2003). All four models dynamically predict land surface water and energy fluxes in response to surface meteorological forcing inputs, but they differ in their structural representation of surface and subsurface water, and energy balance processes.

Three of the four models are traditional land surface schemes that model soil moisture dynamics by solving a layer-based formulation of the standard diffusion and gravity drainage equations for unsaturated flow. Mosaic has three soil layers: (i) a thin 2-cm surface layer, (ii) a 148-cm middle layer, and (iii) a 200-cm-thick bottom layer. Noah uses four soil layers of increasing thicknesses of 10, 30, 60, and 100 cm. CLM (as used here) employs a more highly discretized representation of the subsurface with 10 unevenly spaced layers. CLM's layers have thicknesses of 1.75, 2.76, 4.55, 7.5, 12.36, 20.38, 33.60, 55.39, 91.33, and 113.7 cm, respectively.

The Catchment LSM, by contrast, is nontraditional, in that the vertical soil moisture profile is determined through deviations from the equilibrium soil moisture profile between the surface and the water table. Soil moisture in a 2-cm surface layer and a 100-cm root-zone layer is then diagnosed from the modeled soil moisture profile. The Catchment model includes an explicit treatment of the horizontal variation of soil water and water table depth within each hydrological catchment based on topographic variations within the catchment. The Catchment model is typically used with hydrologically defined catchments (or watersheds) as basic computational units. For ease of model intercomparison, however, the Catchment LSM is used on a regular latitude–longitude grid in this study.

For the remainder of the paper and for clean comparison of output across LSMs, we define root-zone soil moisture as the soil moisture content in the top 1 m of the soil column, regardless of the LSM and its (potentially different) native definition of the term. In other words, our root-zone moisture content is derived as a suitably weighted vertical average over the model layers that are within the top 1 m of the soil column. By contrast, we refer to surface soil moisture as the topmost layer of each model. The specific layer depth for surface soil moisture is 2 cm for Catchment and Mosaic, 1.75 cm for CLM, and 10 cm for Noah.

b. Ensemble Kalman filter

The EnKF is widely used as an effective technique for soil moisture assimilation (Reichle et al. 2002a,b; Crow and Wood 2003; Zhou et al. 2006). The EnKF provides a flexible approach for incorporating errors into the model and the observations. Its ensemble-based treatment of errors makes it suitable for handling the modestly nonlinear dynamics and the temporal discontinuities that are typical of land surface processes. We employ the EnKF approach in all the experiments presented in this article.

The EnKF alternates between an ensemble forecast step and a data assimilation update step (Reichle et al. 2002b). In the forecast step, an ensemble of model states is propagated forward in time using the land surface model. In the update step at time k, this model forecast is adjusted toward the observation based on the relative uncertainties, with appropriate weights expressed in the "Kalman gain" $\mathbf{K}_k$:

$$\mathbf{x}_k^{i+} - \mathbf{x}_k^{i-} = \mathbf{K}_k(\mathbf{y}_k^i - \mathbf{H}_k\mathbf{x}_k^{i-}). \tag{1}$$

The state and (suitably perturbed) observation vectors are represented by $\mathbf{x}_k$ and $\mathbf{y}_k$, respectively. The observation operator $\mathbf{H}_k$ relates the model states to the observed variable. The superscripts $i-$ and $i+$ refer to the state estimates of the ith ensemble member before $(-)$ and after $(+)$ the update, respectively. Put differently, Eq. (1) states that the analysis increments $(\mathbf{x}_k^{i+} - \mathbf{x}_k^{i-})$ are computed by multiplying the innovations $(\mathbf{y}_k^i - \mathbf{H}_k\mathbf{x}_k^{i-})$ with the Kalman gain $\mathbf{K}_k$. The Kalman gain, in turn, is computed from the observation error covariance $\mathbf{R}_k$ and the forecast error covariance $\mathbf{P}_k^-$ (diagnosed as the sample covariance of the ensemble of model forecasts):

$$\mathbf{K}_k = \mathbf{P}_k^-\mathbf{H}_k^{\mathrm{T}}[\mathbf{H}_k\mathbf{P}_k^-\mathbf{H}_k^{\mathrm{T}} + \mathbf{R}_k]^{-1}. \tag{2}$$

Notice that the key term $\mathbf{P}_k^-\mathbf{H}_k^{\mathrm{T}}$ is the cross covariance between errors in the model states (e.g., surface and root-zone soil moisture) and errors in the observed variable (i.e., surface soil moisture), whereas the term in square brackets in Eq. (2) is essentially a normalization factor.

The successive model propagation and update steps imply that surface information is propagated into the root zone in two distinct ways. First, during the model propagation step, soil moisture is exchanged between the surface and deeper layers according to the modeled soil moisture dynamics, typically diffusion and gravity drainage. Second, whenever a surface soil moisture observation is available, an increment to deeper-layer soil moisture is computed and applied in the EnKF update step, based on the surface innovation and the surface-root-zone error correlation (as expressed in the Kalman gain). Given the time scales of soil moisture processes and the fact that the observed surface layer is typically thin compared to deeper soil column reservoirs, the propagation of surface information solely through vertical model physics is relatively inefficient. By contrast, the updating of deeper-layer soil moisture based on the

modeled surface–root zone error correlations (expressed in the ensemble) can provide for an efficient downward propagation of surface information, as long as errors in the surface layer are statistically connected to errors in deeper layers via the model physics.

3. Experiment setup

a. Experiment overview

We designed a suite of synthetic experiments to investigate the influence of model representation of vertical water transport on assimilation performance. The basic structure of the experiments is as follows: A land surface model is selected and an ensemble integration (without data assimilation) is conducted. Each member of the ensemble experiences a different realization of synthetic errors in the forcing inputs and the model prognostic variables (discussed later). From this ensemble, a single realization (or ensemble member) is chosen and assumed to represent the ''true'' state of the land surface, referred to as the control (or truth) run. This synthetic truth serves two purposes: (i) a subset of the truth surface soil moistures, consistent with satellite retrieval availability, is isolated, corrupted with synthetic observation errors and then used for assimilation into the available land surface models; and (ii) the soil moistures produced in this truth, or ''control,'' simulation are used to evaluate the accuracy of subsequent model integrations that assimilate synthetic observations generated from this truth. The mean over all members of the ensemble integration represents the ''open loop'' simulation and represents the model skill without the benefit of data assimilation. These steps are repeated for each of the four LSMs, yielding four different sets of truth data, synthetic observations, and open loop estimates.

Next, a given set of synthetic observations is assimilated into each of the four land surface models with the EnKF (section 2b), resulting in four sets of data assimilation products. Under our original assumption that a single member of the open loop LSM simulation (corresponding to the chosen set of synthetic observations) serves as truth, we can then compute the skill with which the four assimilation integrations approximate the truth data. For a given model, the skill found for the assimilation product minus that for the corresponding open loop product is our metric of interest (section 3c); this difference is the skill improvement associated with data assimilation. The process is then repeated, taking a simulation from a different model as truth and assimilating the corresponding synthetic observations into each of the four LSMs. After each of the four models serves in turn as truth, we end up with a 4×4 matrix of skill improvement associated with data assimilation. The columns of the matrix represent the different versions of truth. Each row of the matrix corresponds to a specific model used for assimilation, showing how assimilation improves its product relative to its open loop product under different versions of truth.

Note that for a given assumed truth, one of the four model experiments is an ''identical twin'' experiment, meaning that the model providing the truth is the same as that used in the assimilation integration. The other three experiments are referred to as ''fraternal twin'' experiments because they use an LSM in the assimilation system that is different from that which was used to generate the synthetic truth data for these experiments. This distinction is important in interpreting the matrix of results.

b. Experiment details

All model and assimilation integrations are conducted over a gridded domain that roughly covers the conterminous United States (CONUS; from 30.5°N, 124.5°W to 50.5°N, 75.5°W) at 1° spatial resolution. The LSMs are driven with meteorological forcing data from the Global Data Assimilation System (GDAS); the global meteorological weather forecast model of the National Centers for Environmental Prediction (Derber et al. 1991). First, the models are spun up by cycling 3 times through the period from 1 January 2000 to 1 January 2007. This ensures that the internal model prognostic states have adequate time to reach an equilibrium consistent with the model climatology, meteorological forcing, and parameters. All model and assimilation integrations are conducted over the same 7-yr period. To avoid potential assimilation-related spin-up effects, only data for the 6-yr period from 1 January 2001 to 1 January 2007 are used in the subsequent analysis.

Each open loop or assimilation experiment with a given model consists of 12 ensemble members (Kumar et al. 2008b), and all data assimilation estimates are based on taking a mean of the ensemble. The ensemble members differ from each other in two ways: (i) noise is added to the meteorological forcing and (ii) noise is added to the model prognostic fields. The parameters used for these perturbations are listed in Tables 1a–1e. Zero-mean, normally distributed additive perturbations are applied to the downward longwave radiation (LW) forcing, and lognormal multiplicative perturbations with a mean value of 1 are applied to the precipitation (P) and downward shortwave radiation (SW) fields (Table 1a). Time series correlations are imposed via a first-order regressive model [AR(1)] with a time scale of 24 hours. No spatial correlations are applied because this study uses the one-dimensional version of the EnKF (Reichle

TABLE 1. (a) Perturbation parameters for SW, LW, and P forcings. (b) Perturbation parameters for Cat model prognostic variables. Cross correlations are not imposed. (c) Perturbation parameters for Mos sm prognostic variables. Variable sm_1 represents top-most layer. (d) Same as (c) but for Noah. (e) Same as (c) but for CLM.

Variable	Std dev	Cross correlations with perturbations		
		SW	LW	P
SW	0.30 (−)	1.0	−0.5	−0.8
LW	50 W m^{-2}	−0.5	1.0	0.5
P	0.50 (−)	−0.8	0.5	1.0

Variable	Std dev (mm)
Catchment deficit	0.14
Surface excess	0.03

Variable	Std dev (m^3 m^{-3})	Cross correlations with perturbations		
		sm_1	sm_2	sm_3
sm_1	1.70E-3	1.0	0.6	0.3
sm_2	1.50E-4	0.6	1.0	0.6
sm_3	1.00E-4	0.3	0.6	1.0

Variable	Std dev (m^3 m^{-3})	Cross correlations with perturbations			
		sm_1	sm_2	sm_3	sm_4
sm_1	6.00E-3	1.0	0.6	0.4	0.2
sm_2	1.10E-4	0.6	1.0	0.6	0.4
sm_3	6.00E-5	0.4	0.6	1.0	0.6
sm_4	4.00E-5	0.2	0.4	0.6	1.0

Variable	Std dev (m^3 m^{-3})	Cross correlations with perturbations									
		sm_1	sm_2	sm_3	sm_4	sm_5	sm_6	sm_7	sm_8	sm_9	sm_{10}
sm_1	1.00E-3	1.0	0.7	0.7	0.6	0.6	0.6	0.6	0.4	0.4	0.4
sm_2	7.00E-4	0.7	1.0	0.7	0.7	0.6	0.6	0.6	0.6	0.4	0.4
sm_3	5.00E-4	0.7	0.7	1.0	0.7	0.7	0.6	0.6	0.6	0.6	0.4
sm_4	3.00E-4	0.6	0.7	0.7	1.0	0.7	0.7	0.6	0.6	0.6	0.6
sm_5	2.00E-5	0.6	0.6	0.7	0.7	1.0	0.7	0.7	0.6	0.6	0.6
sm_6	2.00E-5	0.6	0.6	0.6	0.7	0.7	1.0	0.7	0.7	0.6	0.6
sm_7	2.00E-5	0.6	0.6	0.6	0.6	0.7	0.7	1.0	0.7	0.7	0.6
sm_8	1.50E-6	0.4	0.6	0.6	0.6	0.6	0.7	0.7	1.0	0.7	0.7
sm_9	1.50E-6	0.4	0.4	0.6	0.6	0.6	0.6	0.7	0.7	1.0	0.7
sm_{10}	5.00E-8	0.4	0.4	0.4	0.6	0.6	0.6	0.6	0.7	0.7	1.0

and Koster 2003). Cross correlations are imposed on the perturbations of radiation and precipitation fields using the values specified in Table 1a.

Model prognostic variables for each LSM are perturbed with additive noise, with additional vertical correlations imposed on the perturbations for the Noah, CLM, and Mosaic LSMs' prognostic variables. The parameters for the Catchment LSM (Table 1b) are based on the values of Reichle et al. (2008). The parameters for the other land surface models (Tables 1c–1e) are designed to yield comparable ensemble spreads and comparable open loop skills. For all model prognostic perturbations, we impose AR(1) time series correlations with a 12-h time scale. Further, it was also ensured that these error settings do not introduce systematic biases in the truth and open loop integrations relative to the standard, unperturbed model integrations.

For the assimilation experiments, the synthetic soil moisture retrievals require some special preprocessing. To account for difficulties in retrieving soil moisture products from microwave sensors, the synthetic observations are masked out for high vegetation density (specifically, when the green vegetation fraction values used in Noah exceed 0.7). Also, the soil moisture "observations" are masked out when snow is present on the ground, the soil is frozen, and during precipitation events to mimic the difficulty of retrieving soil moisture during these events. The data masks for snow and frozen soil are generated based on the snow cover and soil temperature values from the control integrations of all four models. Further, random Gaussian noise with an error standard deviation of 0.03 m^3 m^{-3} (volumetric soil moisture) is added to the synthetic observations to mimic measurement uncertainty.

Data assimilation methods (including the EnKF) are designed to correct random errors in the model background and assume that model and observations are climatologically unbiased. The climatologies of the model and satellite estimates, however, are typically very different, as are the climatologies of estimates from different land surface models. Such climatological biases must be addressed as part of the assimilation experiment. Here, we adopt the a priori scaling method of Reichle and Koster (2004). In this approach, the observations are scaled to the model's climatology so that the cumulative distribution functions (CDFs) of the observations and the model match (for each grid point). The scaling of observations is performed prior to each assimilation experiment (except for identical twin experiments, for which this scaling is not necessary because the observations are generated from the same land surface model that is used in the assimilation integration). CDF matching can be used with new satellite sensors only after robust CDF estimates have been obtained. Reichle and Koster (2005) show that data records of one year are adequate.

c. *Evaluation metric: Normalized information contribution*

Because the observations are scaled prior to the assimilation experiment, the anomaly time series correlation (rather than RMSE) is used quantify the skill of the estimates. This anomaly time series is obtained (for each grid point) as follows. We subtract the monthly-mean climatology of each dataset from the corresponding daily

average raw data, so that the anomalies represent the daily deviations from the mean seasonal cycle. Therefore, we do not take advantage of the "skill" inherent in the seasonal cycle. Subsequently, we compute the time series correlation coefficient between the daily anomaly estimates and the corresponding anomalies of the truth data, at each grid point. Note that only grid points with a minimum of 600 valid observations for the evaluation period are included in the comparisons.

To evaluate improvements due to assimilation, a normalized information contribution (NIC) metric is computed as follows: the monthly anomaly time series coefficients R_a for the assimilation and R_o for the open loop integrations are computed. A normalized information contribution is then defined as NIC = $(R_a - R_o)/(1 - R_o)$, which is a measure of how much of the maximum skill improvement $(1 - R_o)$ is realized through data assimilation $(R_a - R_o)$. Assuming that the assimilation product is no worse than the model-only output $(R_a > R_o)$, we have $0 \leq \text{NIC} \leq 1$. For NIC = 0, the assimilation of surface soil moisture does not add any information to the assimilation product, and for NIC = 1, the assimilation realizes the maximum skill improvement possible. The NIC metric is needed primarily because it is extremely difficult—if not impossible—to achieve identical open loop skill for different LSMs for all the 16 assimilation simulations. Hereinafter, we also refer to the NIC metric loosely as the "skill improvement" through data assimilation.

4. Results and discussion

Before analyzing the contribution of the surface retrievals in the data assimilation system, it is informative to take a closer look at how surface soil moisture is connected to root-zone soil moisture in the four LSMs, and how errors in the surface layer are connected to errors in the root zone.

a. Vertical coupling strength and gain correlation

As discussed earlier, each land surface model possesses a different representation of soil moisture dynamics based on its particular parameterizations of soils and vegetation properties, and processes related to the partitioning of rainfall into infiltration, runoff, and evaporation components. As a result, the coupling between the surface and subsurface soil moisture is different in each LSM. One way of measuring the vertical coupling strength is through correlating soil moisture anomalies in the surface layer with anomalies in root-zone soil moisture. More precisely, we define the (spatially distributed) "native vertical coupling strength" as the anomaly correlation coefficient between surface and root-zone soil moisture time series, for a given truth model integration without data assimilation. Put differently, the native vertical coupling strength measures the degree to which a positive (negative) anomaly in surface soil moisture coincides with a positive (negative) anomaly in the root zone.

This native vertical coupling strength is shown in Fig. 1 for each of the four LSMs, by only including the locations and times at which surface soil moisture retrievals are available. Our subsequent analysis of the data assimilation performance follows a similar strategy, meant to characterize the skill improvements only at observation times and locations. Figure 1 shows that the surface and root-zone soil moisture are most tightly coupled in the Catchment model, followed by Mosaic and Noah. CLM has the weakest coupling strength, possibly as a result of its use of the most soil layers. In other words, for soil moisture produced by the Catchment model, knowledge of a surface anomaly is more informative about root-zone anomalies (at a given point in time) than for the other LSMs. Across all models, the native vertical coupling strength tends to be somewhat larger in the south and in the east of the domain, which is likely influenced by the generally wetter climate and the relative absence of cold-season processes. Note again that we only compare the coupling strength between different models, and we do not claim that a particular model has the least or most realistic representation of the coupling strength that occurs in nature.

The native coupling strength is an important metric that diagnoses the connection between surface and root-zone soil moisture. It does not, however, directly measure how much a surface observation contributes to an update of root-zone soil moisture in the EnKF. The surface–root zone connection in the data assimilation update is based on the modeled error correlations and can be diagnosed by a closer look at the Kalman gain. In the assimilation update step, the EnKF method computes analysis increments for surface and root-zone soil moisture based on the Kalman gain and the innovations [Eqs. (1) and (2)]. Because we use a "one dimensional" EnKF (Reichle and Koster 2003), the observations are effectively scalars and the gain is a vector. The element K_j of the gain that corresponds to a particular (model specific) soil moisture layer j is thus directly proportional to the error covariance between the model forecast soil moisture in the surface layer and that in layer j, labeled x_{sf} and x_j, respectively:

$$K_j \propto \text{cov}(x_{\text{sf}}^-, x_j^-). \tag{3}$$

The K_j's can easily be calculated from the ensemble at each update time during each assimilation integration.

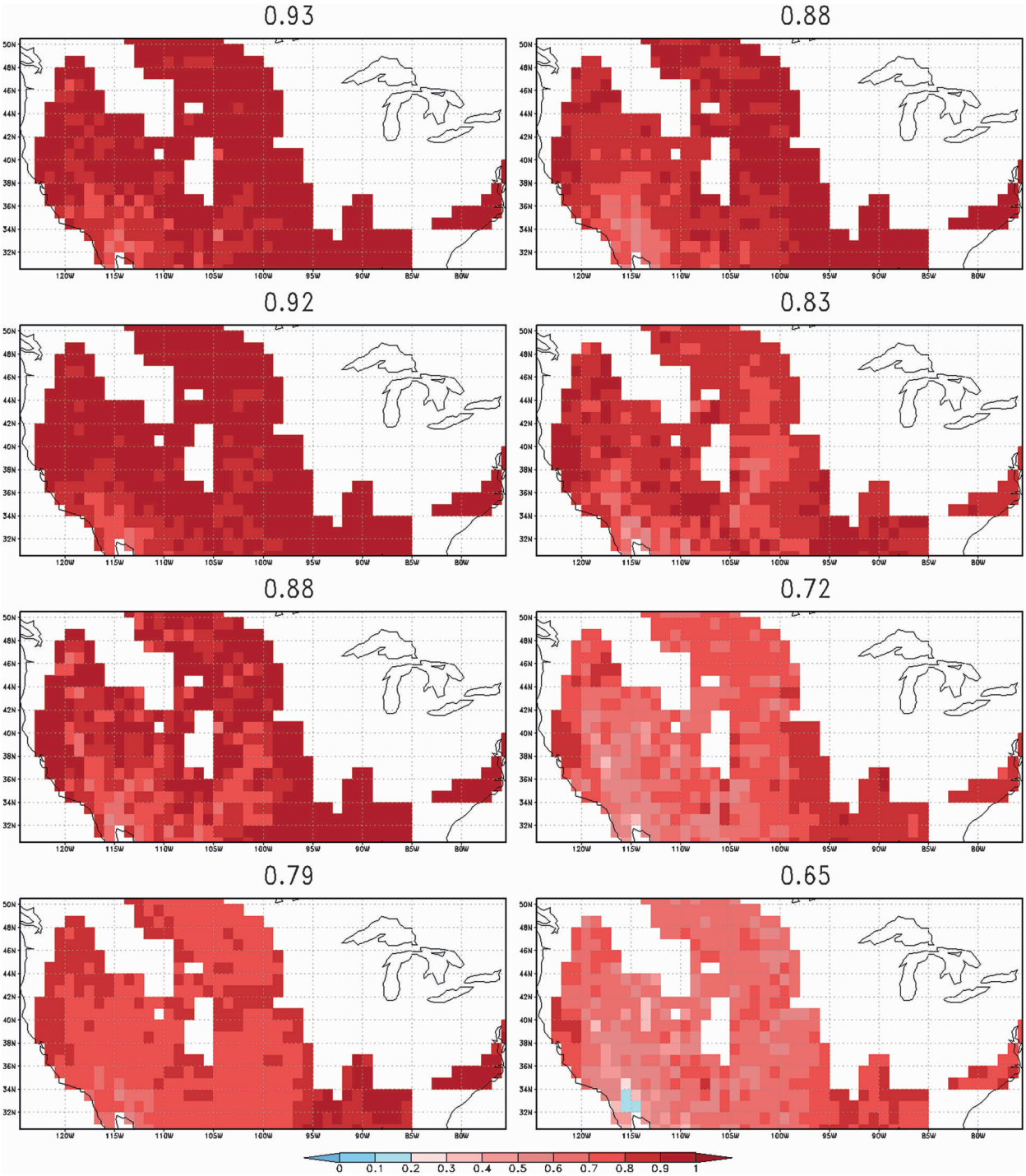

FIG. 1. (left) Anomaly time series correlation coefficient (native VCS) between surface and root-zone sm and (right) time average gain correlations from the assimilation experiments for (from top): Cat, Mos, Noah, and CLM. Numbers above show domain averaged values.

Next, we compute a (spatially distributed) scalar root-zone gain K_{rz} for the top 100-cm root-zone layer through model-specific vertical averaging of the K_j's. Hereinafter, K_{rz} is referred to as the "gain correlation" metric. It is determined primarily by the model physics and by our choice of perturbation input parameters (in particular, the vertical correlations in the perturbations to the soil moisture states listed in Tables 1b–1e). Most importantly,

TABLE 2. NIC of assimilated surface sm to skill in surface sm anomalies. Columns indicate which LSM is used in the generation of the synthetic truth and retrievals, and rows indicate which model is used to assimilate the synthetic retrievals. Last row and column indicate averages across all models.

	Truth				
Surface	Cat	Mos	Noah	CLM	Avg
Cat	0.71	0.44	0.39	0.33	0.47
Mos	0.43	0.59	0.54	0.57	0.53
Noah	0.40	0.44	0.53	0.45	0.46
CLM	0.37	0.52	0.45	0.67	0.50
Avg	0.48	0.50	0.48	0.49	

TABLE 3. Same as Table 2 but for root-zone sm NIC values.

	Truth				
Root zone	Cat	Mos	Noah	CLM	Avg
Cat	0.72	0.54	0.37	0.38	0.50
Mos	0.55	0.70	0.32	0.34	0.48
Noah	0.44	0.36	0.44	0.26	0.38
CLM	0.11	0.22	0.11	0.45	0.22
Avg	0.46	0.48	0.29	0.36	

the gain correlation directly indicates the size of the root-zone increment that results from a unit innovation and measures by how much a surface observation affects adjustments of root-zone soil moisture through the EnKF update.

Figure 1 also shows the time-average gain correlation for each LSM (averaged over the four assimilation experiments for which the given LSM was used in the assimilation system). The gain correlation trends are similar to the trends observed in the native vertical coupling strengths of each LSM, with Catchment having the highest value and Mosaic, Noah, and CLM having successively lower values. Across all models, the gain correlations exhibit slightly larger values in the southern and eastern parts of the domain. The comparison of the vertical coupling strength and gain correlations in Fig. 1 suggests that in assimilation integrations using a LSM with strong surface–root zone coupling—Catchment or Mosaic, for example—root-zone increments tend to correlate strongly with surface innovations. Similarly, using a LSM with weaker surface–root zone coupling is likely to produce less correlation between root-zone increments and surface innovations.

b. *Assimilation performance*

Let us now turn to the analysis of skill improvement through assimilation of surface observations. Tables 2 and 3 list the skill improvement (as domain-averaged NIC values, section 3c) for the surface and root-zone soil moisture products, respectively. As mentioned earlier, the NIC values are computed using anomalies at times and locations for which surface soil moisture retrievals are available, representing skill improvements relative to possible observation instances.

Each table presents the domain-averaged NIC values obtained from all 16 assimilation experiments, constituting the 4×4 matrix of skill improvements described in section 3. Again, the diagonal elements of this matrix represent the identical twin experiments and the off-diagonal elements represent the fraternal twin experiments. Note first that the skill improvements from the identical twin experiments are generally larger than those from the fraternal twin experiments, for both surface and root-zone products. On average, the NIC values on the diagonal (corresponding to identical twin experiments) exceed the off-diagonal elements of the corresponding fraternal twin experiments by 0.18 for surface soil moisture improvements and by 0.24 for root-zone soil moisture improvements. In a relative sense, identical twin experiments overestimate the skill derived from the assimilation of surface observations by 42% for surface soil moisture estimates and by 71% for root-zone soil moisture estimates. Our first important conclusion is therefore that the identical twin experiments significantly overestimate the benefits derived from data assimilation relative to the fraternal experiments, which are more likely to represent the assimilation of actual satellite observations.

Each column of Tables 2 and 3 represents the benefit of surface soil moisture assimilation under a given scenario of true soil moisture physics, as obtained from different model representations. Correspondingly, the rows of Tables 2 and 3 measure the improvements from assimilation of surface observations into a particular LSM for a range of potential truths. If one assumes that each synthetic truth is equally likely, the mean over the row values represents an "expected value of skill improvement" in a data assimilation system that uses a particular LSM as its land model component. We have no way, of course, of justifying the assumption of equal likelihood here. We can say, though, that the spreads in the averages are larger for Table 3 than for Table 2, suggesting that although the ability of the LSMs to generate surface soil moisture information is comparable, model skill with regard to capturing root-zone information varies significantly.

In conjunction with Fig. 1, Tables 2 and 3 suggest that the skill improvements in the root zone for a given location can be represented as a function of two factors: (i) the vertical coupling strength of the model used to generate the truth (hereafter VCS-truth) and (ii) the vertical coupling strength of the model used in the assimilation system (hereafter VCS-assimilation). To investigate

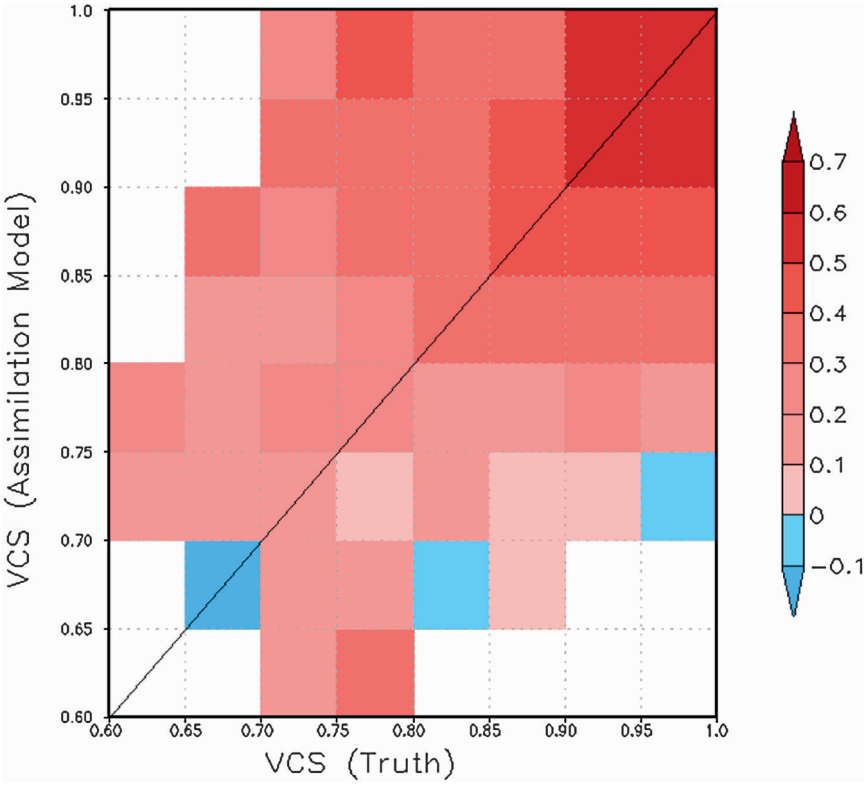

FIG. 2. Root zone normalized information contribution from the fraternal twin assimilation runs as function of the (abscissa) native VCS of the model used for generating VCS-truth and (ordinate) native VCS of the model used in the assimilation integration.

this point further, Fig. 2 stratifies (''bins'') the root-zone NIC values for all spatial locations and for all 12 fraternal twin assimilation integrations based on these two factors. (We exclude the results from the identical twin experiments because they overestimate the skill improvements from data assimilation. If we had included them, only the diagonal points in the figure would change; the values along the diagonal would indeed increase, but the overall trends seen would remain the same.) The diagonal (shown in Fig. 2) from the lower-left corner to the upper-right corner represents the skill improvement values when the VCS-model and VCS-assimilation values are roughly the same. On or off the diagonal, the skill improvements are generally higher for higher values of VCS-truth and VCS-assimilation, as indicated by the upper-right corner in Fig. 2.

This result is intuitive. Recall from Fig. 1 that Catchment and Mosaic LSMs exhibit higher positive gain correlations than Noah and CLM LSMs, which implies that positive surface soil moisture innovations in Catchment and Mosaic lead to correspondingly positive increments in the root zone. Now recall that there is a strong correlation between the surface and root-zone soil moisture in the Catchment and Mosaic LSMs (as measured by each model's native coupling strength; Fig. 1). When the LSMs with strong VCS serve as the truth, the assimilation system tends to produce root-zone increments with the appropriate sign. This implies that the assimilation system does not need to rely as much on the less efficient process of propagating the surface increments into the root zone through the model physics. In other words, stronger vertical coupling makes it easier for the assimilation system to infer the root-zone estimates from the surface information. This trend is also consistent with Table 3, where the column averages of NICs are higher for Catchment and Mosaic truths, which have stronger vertical coupling strengths than Noah and CLM truths.

Simply put, if truth and the model in the assimilation system both show a strong connection between the surface and root zone (i.e., a strong VCS), surface information is more efficiently transferred to the root zone, increasing the skill scores. Figure 2 serves to quantify this intuitive result with an ensemble of models and data assimilation techniques.

The trends in Fig. 2 also indicate a slight asymmetry in the NIC surface with the upper triangular area (relative to the lower left–upper right diagonal) showing higher

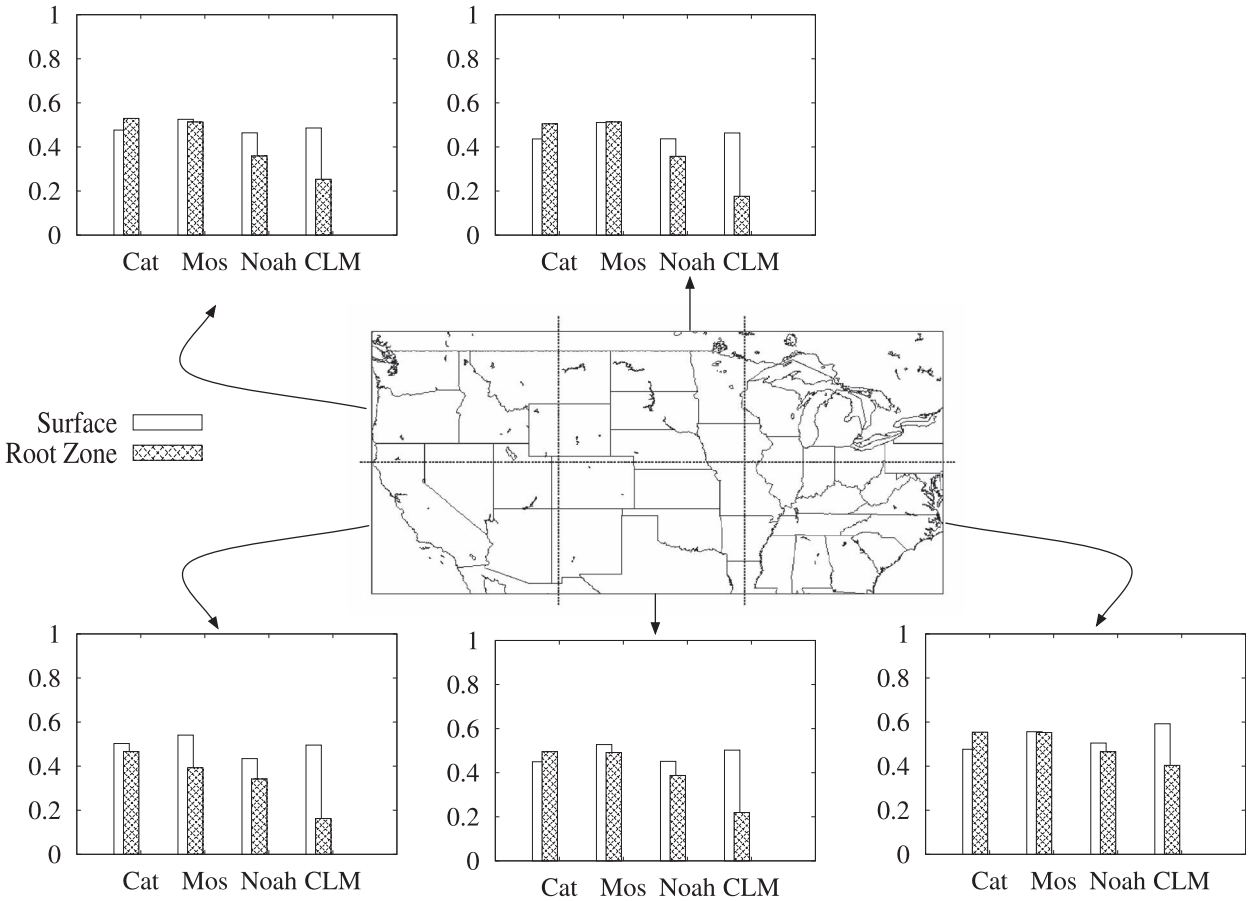

FIG. 3. NIC by geographic regions for Cat, Mos, Noah, and CLM.

NIC values than the lower triangular area. This implies that, for a given VCS-truth, the use of a model with higher native VCS-assimilation tends to produce stronger skill improvements. This suggests that unless it is clear that a weak surface–root zone representation is the best modeling strategy, it is prudent to use a LSM with strongly coupled surface and root zone in the data assimilation. It must be noted that this inference is a direct result of the inclusion of CLM in the analysis. As evident from Table 3, the NIC values tend to be lower in the fraternal twin experiments with CLM as the assimilation model. We speculate that the highly discretized soil profile representation of CLM contributes to its relatively lower VCS. This hypothesis can be tested by changing the layering structure of a LSM and is left for a future research study. When CLM is excluded from the previously mentioned analysis, the asymmetry is no longer observed in Fig. 2. (Again, our analysis does not suggest that CLM represents natural processes particularly well or particularly poorly.) Another interesting trend to note is that the even when the assimilation model overestimates the truth vertical coupling strength by up to 0.1, the skill improvements from assimilation still shows an increase as the VCS-truth increases.

To compute the statistical significance of the NIC values, the 99% confidence intervals of the anomaly time series correlation coefficients for the assimilation (δR_a) and the open loop integrations (δR_o) are translated into a corresponding 99% confidence interval for the NIC values (δNIC) using Eq. (4):

$$\delta\mathrm{NIC} = \delta R_a \frac{1}{(1 - R_o)} + \delta R_o \frac{(R_a - 1)}{(1 - R_o)^2}. \qquad (4)$$

Using this formulation, the 99% confidence intervals computed for the NIC values provide a range of approximately ± 0.002, indicating a high level of statistical significance in the skill improvement trends presented in Fig. 2 and Tables 2 and 3.

The dependence of the skill improvements from the assimilation runs to different climate regions is examined by stratifying the domain geographically. Figure 3 shows the average NIC values from different LSMs (averaged over the rows of the 4×4 matrix as in the

''unknown truth'' scenario) for five different geographic regions. (Notice that the region in the northeast location is omitted because there are not enough valid observation retrievals in this area). For each LSM, the trends in the skill improvements are similar across the five regions. In Catchment and Mosaic LSMs, the magnitude of skill improvements in the root zone is comparable to the improvements in surface soil moisture, whereas for Noah and CLM, the root-zone skill improvements are smaller than the surface skill improvements. This trend is consistent with our earlier result that models with strong vertical coupling are likely to generate root-zone skill improvements more strongly correlated with surface skill improvements. In the three southern regions, the skill improvements generally increase going from west to east, consistent with the generally drier climate in the west compared to the generally wetter climate in the east. The wetter conditions lead to more tightly coupled surface and root-zone conditions, which are easier to replicate, as evident in Fig. 2. Further, the skill improvements in the northern regions are marginally lower than the corresponding values in the southern regions. This could be due to the additional interaction of cold-season processes and soil moisture dynamics, which may lead to a decoupling of the surface and root-zone soil moisture for part of the year.

The strength of coupling between different soil layers is also influenced by the soil texture types used in the models (Capehart and Carlson 1997). Figure 4 shows a comparison of NIC values stratified according to the soil texture types in the domain. The skill improvements corresponding to sandier soils (loamy sand, sandy loam, sandy clay loam) are smaller than the improvements in clayey soils (loam, clay loam, clay). The clayey soils exert stronger capillary forces than sandy soils, and therefore they show more tightly correlated surface and root-zone improvements in all LSMs.

5. Summary

Here we investigate the effect of various land surface model physics on soil moisture products derived through the assimilation of surface soil moisture retrievals. In the assimilation system, observed surface information is propagated into deeper soil layers, giving the surface retrievals an otherwise unobtainable relevance to such applications as the initialization of weather and seasonal climate forecasts. Because the LSMs differ significantly in their representation of subsurface water dynamics, the downward propagation of the surface information in the assimilation system strongly depends on which LSM is used as the system's model component. Here we study how the specific formulation of the LSM that is used in

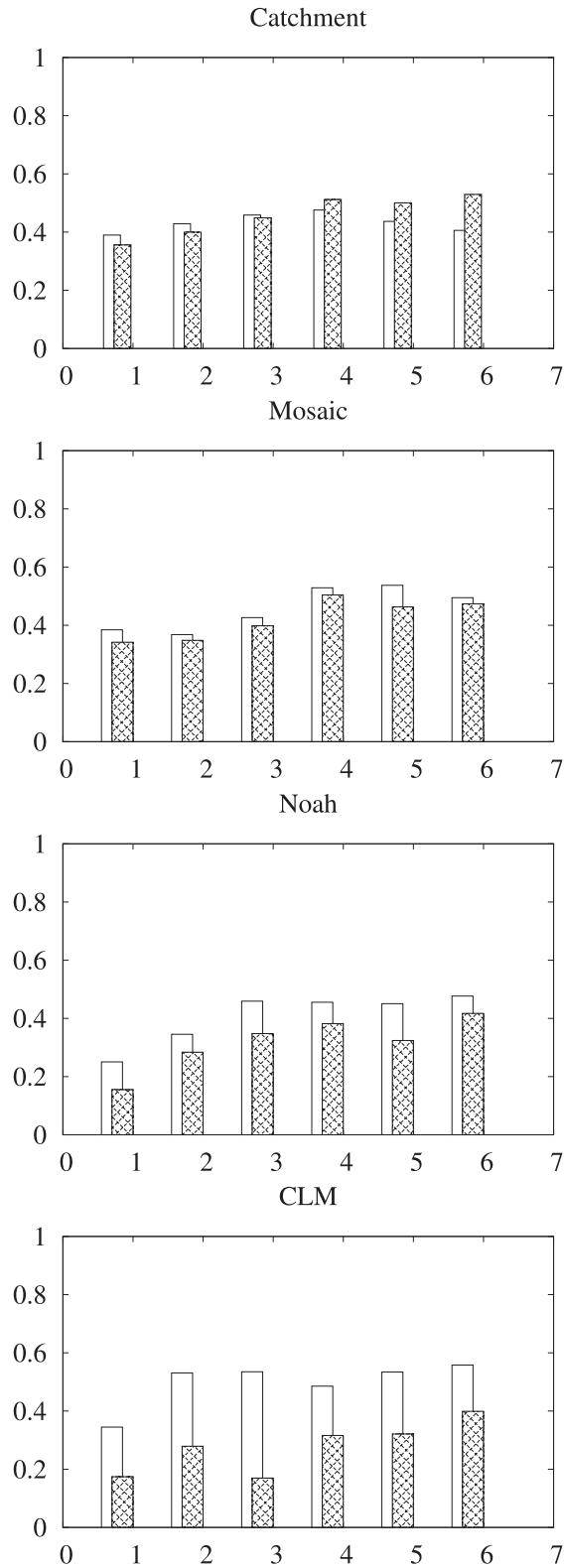

FIG. 4. NIC by soil texture—1: loamy sand; 2: sandy loam; 3: sandy clay loam; 4: loam; 5: clay loam; 6: clay—for (top to bottom) Cat, Mos, Noah, and CLM.

the assimilation system affects the information contribution to soil moisture assimilation products.

The experiments presented in this article were conducted with the Catchment, Mosaic, Noah, and CLM land surface models and the EnKF data assimilation algorithm. The modeling domain roughly covers the continental United States for a 6-yr period. The LSMs vary in complexity in their representation of subsurface soil moisture dynamics. The Catchment LSM essentially describes deviations from the equilibrium soil moisture profile and has a relatively strong vertical coupling between the surface and root-zone soil moisture. By contrast, the layer-based models Mosaic (3 layers), Noah (4 layers), and CLM (10 layers) have successively weaker coupling between their surface and root zones.

Our synthetic experiments consisted of assimilating each of four synthetic retrievals datasets (based on integrations of each of the four LSMs) into four separate EnKF-based assimilation systems that use the four LSMs as their model component. The resulting 16 assimilation soil moisture products were evaluated against the corresponding synthetic truth datasets and compared to corresponding model integrations without the benefit of data assimilation. This information was summarized in a skill improvement metric that measures the normalized information contribution of the surface soil moisture retrievals to the skill of the soil moisture assimilation products (relative to the maximum possible improvement). This experiment setup allowed us to investigate the information contribution under a variety of combinations of possible true soil moisture dynamics with assimilation systems that use a range of LSMs.

The results clearly demonstrate that the assimilation of surface soil moisture provides improvements in the root-zone estimates. The magnitude of the improvements depends on the LSM that is used in the assimilation system and on the (synthetic) true subsurface physics (i.e., on the LSM that is used to generate the synthetic truth and the corresponding synthetic retrievals). Generally, identical twin experiments tend to overestimate skill improvements when compared to those of more realistic fraternal twin experiments. Likewise, the potential for improvements in the root zone is generally higher if the true subsurface physics exhibits a strong correlation between the surface and root zone, especially if the assimilation model also shows such a strong correlation. For weaker surface–root zone coupling strength, surface soil moisture assimilation yields more limited improvements in the root zone.

The results also provide insights into the optimal choice of LSM for soil moisture assimilation when the true subsurface physics is essentially unknown. An LSM with a strongly coupled representation of the surface and subsurface is perhaps a more robust choice for assimilation, unless independent information suggests that the use of a LSM with a more decoupled surface–subsurface representation is more realistic. We must emphasize here, however, that appropriate independent information (e.g., from soil moisture observations) is essentially unavailable. Point measurements of soil moisture exist but are not necessarily representative of large-scale vertical coupling strength. At large scales, the connection between the surface and root zone must be controlled in part (and probably enhanced) by lateral flow induced by topography and must, in any case, be affected by spatial heterogeneity in surface properties. Arguably, the ''true'' vertical coupling strength in nature for large-scale areas is unknown at this time.

The improvements in the soil moisture products through assimilation were found to be sensitive to the local climate and also to the soil types used in the land surface models, which can in turn be explained by the dependence of the models' vertical coupling strength on soil type and regional climate. A statistical analysis of the computations demonstrates a high degree of statistical significance in the skill improvement values, and correspondingly in the trends demonstrated in the article.

The comparison of the performance of different land surface models in response to the assimilation of surface soil moisture observations presented in this study is enabled by the LIS framework, which provides a unique environment for such a uniform intercomparison. The capabilities in LIS to use different forcing datasets, observations, and land surface models in an interoperable manner has enabled the rapid specification, calibration, and application of the land surface models for data assimilation. The methodology demonstrated here with the LIS framework can be used as a guideline to evaluate the feasibility of using a land surface model for soil moisture assimilation. The procedure also provides a way to generate realistic measures of skill improvements from soil moisture assimilation, different from the identical twin experiment setup typically used to calibrate the assimilation system. Lastly, the insights obtained on each model's performance through this study is expected to aid in their application for real assimilation experiments.

Acknowledgments. This research was partly supported by an internal investment grant from the NASA Goddard Space Flight Center. We also acknowledge the support from the Air Force Weather Agency, which funded the development of data assimilation capabilities in LIS. Rolf Reichle was partly supported through NASA Grants NNG05GB61G and NNX08AH36G. Computing was supported by the NASA High-End

Computing Program; we gratefully acknowledge this support.

REFERENCES

Calvet, J.-C., J. Noilhan, and P. Bessemoulin, 1998: Retrieving root-zone soil moisture from surface soil moisture of temperature estimates: A feasibility study based on field measurements. *J. Appl. Meteor.,* **37,** 371–386.

Capehart, W., and T. Carlson, 1997: Decoupling of surface and near-surface soil water content: A remote sensing perspective. *Water Resour. Res.,* **33,** 1383–1395.

Chen, F., and R. Avissar, 1994: The impact of land-surface wetness heterogeneity on mesoscale heat fluxes. *J. Appl. Meteor.,* **33,** 1323–1340.

Crow, W. T., and E. F. Wood, 2003: The assimilation of remotely sensed soil brightness temperature imagery into a land surface model using ensemble Kalman filtering: A case study based on ESTAR measurements during SGP97. *Adv. Water Resour.,* **26,** 137–149.

Dai, Y., and Coauthors, 2003: The Common Land Model (CLM). *Bull. Amer. Meteor. Soc.,* **84,** 1013–1023.

Derber, J., D. Parrish, and S. Lord, 1991: The new global operational analysis system at the National Meteorological Center. *Wea. Forecasting,* **6,** 538–547.

Drusch, M., 2007: Initializing numerical weather prediction models with satellite-derived surface soil moisture: Data assimilation experiments with ECMWF's Integrated Forecast System and the TMI soil moisture data set. *J. Geophys. Res.,* **112,** D03102, doi:10.1029/2006JD007478.

Ek, M., K. Mitchell, L. Yin, P. Rogers, P. Grunmann, V. Koren, G. Gayno, and J. Tarpley, 2003: Implementation of Noah land surface model advances in the National Centers for Environmental Prediction operational mesoscale Eta model. *J. Geophys. Res.,* **108,** 8851, doi:10.1029/2002JD003296.

Engman, E. T., and R. J. Gurney, 1991: *Remote Sensing in Hydrology*. Van Nostrand Reinhold, 225 pp.

Entekhabi, D., H. Nakamura, and E. G. Njoku, 1994: Solving the inverse problem for soil moisture and temperature profiles by sequential assimilation of multifrequency remotely senses observations. *IEEE Trans. Geosci. Remote Sens.,* **32,** 438–448.

Heathman, G. C., P. J. Starks, L. R. Ahuja, and T. J. Jackson, 2003: Assimilation of surface soil moisture to estimate profile soil water content. *J. Hydrol.,* **279,** 1–17.

Jackson, T. J., 1986: Soil water modeling and remote sensing. *IEEE Trans. Geosci. Remote Sens.,* **GE-24,** 37–46.

——, 1993: Measuring surface soil moisture using passive microwave remote sensing. *Hydrol. Processes,* **7,** 139–152.

Kerr, Y. H., P. Waldteufel, J.-P. Wigneron, J.-M. Martinnuzzi, J. Font, and M. Berger, 2001: Soil moisture retrieval from space: The soil moisture and ocean salinity (SMOS) mission. *IEEE Trans. Geosci. Remote Sens.,* **39,** 1729–1735.

Koster, R. D., and M. J. Suarez, 1996: Energy and water balance calculations in the mosaic LSM. Tech. Rep. Series on Global Modeling and Data Assimilation, Vol. 9, NASA Tech. Memo. 104606, 69 pp.

——, ——, A. Ducharne, M. Stieglitz, and P. Kumar, 2000: A catchment-based approach to modeling land surface processes in a general circulation model 1. Model structure. *J. Geophys. Res.,* **105** (D20), 24 809–24 822.

——, and Coauthors, 2004: Realistic initialization of land surface states: Impacts on subseasonal forecast skill. *J. Hydrometeor.,* **5,** 1049–1063.

Kostov, K. G., and T. J. Jackson, 1993: Estimating profile soil moisture from surface-layer measurements: A review. *Ground Sensing,* H. N. Nasr, Ed., International Society for Optical Engineering (SPIE Proceedings, Vol. 1941), 125–136.

Kumar, S., and Coauthors, 2006: Land information system: An interoperable framework for high resolution land surface modeling. *Environ. Modell. Software,* **21,** 1402–1415.

——, C. Peters-Lidard, J. L. Eastman, and W.-K. Tao, 2007: An integrated high-resolution hydrometeorological modeling testbed using LIS and WRF. *Environ. Modell. Software,* **23,** 169–181.

——, ——, Y. Tian, R. H. Reichle, J. Geiger, C. Alonge, J. Eylander, and P. Houser, 2008a: An integrated hydrologic modeling and data assimilation framework. *Computer,* **41,** 52–59, doi:10.1109/MC.2008.511.

——, R. Reichle, C. Peters-Lidard, R. Koster, X. Zhan, W. Crow, J. Eylander, and P. Houser, 2008b: A land surface data assimilation framework using the land information system: Description and applications. *Adv. Water Resour.,* **31,** 1419–1432, doi:10.1016/j.advwatres.2008.01.013.

Li, J., and S. Islam, 2002: Estimation of root zone soil moisture and surface fluxes partitioning using near surface soil moisture measurements. *J. Hydrol.,* **259,** 1–14.

Mitchell, K. E., and Coauthors, 2004: The multi-institution North American Land Data Assimilation system (NLDAS): Utilizing multiple GCIP products and partners in a continental distributed hydrological modeling system. *J. Geophys. Res.,* **109,** D07S90, doi:10.1029/2003JD003823.

Montaldo, N., J. D. Albertson, M. Mancini, and G. Kiely, 2001: Robust simulation of root zone soil moisture with assimilation of surface soil moisture data. *Water Resour. Res.,* **37,** 2889–2900.

National Research Council, 2007: *Earth Science and Applications from Space: National Imperatives for the Next Decade and Beyond*. National Academies Press, 428 pp.

Njoku, E. G., and D. Entekhabi, 1995: Passive microwave remote sensing of soil moisture. *J. Hydrol.,* **184,** 101–130.

Oglesby, R. J., 1991: Springtime soil moisture, natural climate variability, and North American drought as simulated by the NCAR Community Climate Model 1. *J. Climate,* **4,** 890–897.

Peters-Lidard, C. D., and Coauthors, 2007: High-performance Earth system modeling with NASA/GSFC's Land Information System. *Innovations Syst. Software Eng.,* **3,** 157–165.

Reichle, R., and R. Koster, 2003: Assessing the impact of horizontal error correlations in background fields on soil moisture estimation. *J. Hydrometeor.,* **4,** 1229–1242.

——, and ——, 2004: Bias reduction in short records of satellite soil moisture. *Geophys. Res. Lett.,* **31,** L19501, doi:10.1029/2004GL020938.

——, and ——, 2005: Global assimilation of satellite surface soil moisture retrievals into the NASA Catchment land surface model. *Geophys. Res. Lett.,* **32,** L02404, doi:10.1029/2004GL021700.

——, D. M. McLaughlin, and D. A. Entekhabi, 2002a: Hydrologic data assimilation with the ensemble Kalman filter. *Mon. Wea. Rev.,* **130,** 103–114.

——, J. Walker, R. Koster, and P. Houser, 2002b: Extended versus ensemble Kalman filtering for land data assimilation. *J. Hydrometeor.,* **3,** 728–740.

——, R. Koster, P. Liu, S. Mahanama, E. Njoku, and M. Owe, 2007: Comparison and assimilation of global soil moisture retrievals

from the advanced Microwave Scanning Radiometer for the Earth Observing System (AMSR-E) and the Scanning Multichannel Microwave Radiometer (SMMR). *J. Geophys. Res.,* **112,** D09108, doi:10.1029/2006JD008033.

——, W. Crow, and C. Keppenne, 2008: An adaptive ensemble Kalman filter for soil moisture data assimilation. *Water Resour. Res.,* **44,** W03423, doi:10.1029/2007WR006357.

Rodell, M., and Coauthors, 2004: The Global Land Data Assimilation System. *Bull. Amer. Meteor. Soc.,* **85,** 381–394.

Schmugge, T. J., T. J. Jackson, and H. L. McKim, 1980: Survey of methods for soil moisture determination. *Water Resour. Res.,* **16,** 961–979.

Trier, S., F. Chen, and K. Manning, 2004: A study of convection initiation in a mesoscale model using high-resolution land surface initial conditions. *Mon. Wea. Rev.,* **132,** 2954–2976.

Walker, J. P., G. R. Willgoose, and J. D. Kalma, 2001: One-dimensional soil moisture profile retrieval by assimilation of near-surface observations: A simplified soil moisture model and field application. *J. Hydrometeor.,* **2,** 356–373.

——, ——, and ——, 2002: Three-dimensional soil moisture profile retrieval by assimilation of near-surface measurements: Simplified Kalman filter covariance forecasting and field application. *Water Resour. Res.,* **38,** 1301, doi:10.1029/2002WR001545.

Zhou, Y., D. McLaughlin, and D. Entekhabi, 2006: Assessing the performance of the ensemble Kalman filter for land surface data assimilation. *Mon. Wea. Rev.,* **134,** 2128–2142.